Efficient Far-Red/Near-IR Absorbing BODIPY Photocages by Blocking Unproductive Conical Intersections

Pradeep Shrestha, Komadhie C. Dissanayake, Elizabeth J. Gehrmann, Chamari S. Wijesooriya, Atreyee Mukhopadhyay, Emily A. Smith*, Arthur H. Winter*

Department of Chemistry, Iowa State University, 1608 Gilman Hall, Ames, Iowa 50010, United States

ABSTRACT: Photocages are light-sensitive chemical protecting groups that give investigators control over activation of biomolecules using targeted light irradiation. A compelling application of far-red/near-IR absorbing photocages is their potential for deep tissue activation of biomolecules and phototherapeutics. Towards this goal, we recently reported BODIPY photocages that absorb near-IR light. However, these photocages have reduced photorelease efficiencies compared to shorter-wavelength absorbing photocages, which has hindered their application. Because photochemistry is a zero-sum competition of rates, improving the quantum yield of a photoreaction can be achieved either by making the desired photoreaction more efficient or by hobbling competitive decay channels. This latter strategy of inhibiting unproductive decay channels was pursued to improve the release efficiency of long-wavelength absorbing BODIPY photocages by synthesizing structures that block access to unproductive singlet internal conversion conical intersections, which have recently been located for simple BODIPY structures from excited state dynamic simulations. This strategy led to the synthesis of new conformationally-restrained boron-methylated BODIPY photocages that absorb light strongly around 700 nm. In the best case, a photocage was identified with an extinction coefficient of 124,000 $M^{-1}cm^{-1}$, a quantum yield of photorelease of 3.8%, and an overall quantum efficiency of 4650 $M^{-1}cm^{-1}$ at 680 nm. This derivative has a quantum efficiency that is 50-fold higher than the best known BODIPY photocages absorbing >600 nm, validating the effectiveness of a strategy for designing efficient photoreactions by thwarting competitive excited state decay channels. Furthermore, 1,7-diaryl substitutions were found to improve the quantum yields of photorelease by excited state participation and blocking ion pair recombination by internal nucleophilic trapping. No cellular toxicity (trypan blue exclusion) was observed at 20 μM, and photoactivation was demonstrated in HeLa cells using red light.

Introduction. Photocages are light-sensitive chemical protecting groups that mask substrates through a covalent linkage that renders the substrate inert.[1] Light irradiation cleaves the protecting group and restores the reactivity or function of the substrate. Photocages are used in chemical, materials, and biological applications that take advantage of the spatial and temporal resolution that that can be provided by light. These applications include photolithographic fabrication of gene chips,[2, 3] light-responsive organic materials and polymers,[4] and protecting groups for use in multistep organic synthesis.[5] In a biological context, these structures are particularly prized for their ability to trigger the release of bioactive molecules upon irradiation. Because it can be focused and pulsed, light provides spatial and temporal resolution that no other external control can match. This control can be exploited to probe the activity of a variety of structures within biological microenvironments including caged proteins,[6, 7] nucleotides, [8-10] ions,[11-16] neurotransmitters,[17, 18] pharmaceuticals,[19, 20] fluorescent dyes,[21, 22] and biological small molecules[23] (e.g., caged ATP).

By far the most popular photocages are the *o*-nitrobenzyl systems [24] and their derivatives, but other photocages that see significant use include those based on the phenacyl,[25] acridinyl,[26] coumarinyl,[27, 28] xanthenyl,[29] ruthenium,[30] and *o*-hydroxynaphthyl structures.[31] A limitation of the most popular photocages is that they absorb light mostly in the ultraviolet region of the optical spectrum where prolonged exposure of cells or tissues to UV light can lead to cell damage or death.

The drawbacks of using UV light has led to a number of different creative approaches to permit photorelease of biologically active substrates using visible light. For example, considerable efforts have been made to red-shift the absorbances of popular photocages beyond the most cell-damaging deep-UV wavelengths and towards the visible,[32, 28] while retaining reasonable photorelease efficiencies. Alternatively, multiphoton absorption methods allow UV-absorbing photocages to be excited with two or more visible light photons.[33, 34] Other methods to achieve photorelease with visible light include photorelease initiated via photoinduced electron transfer,[35-37] via metal–ligand photocleavage,[6, 38, 39] by exploiting internal photoredox reactions of quinones,[40, 41] or by using photosensitizers that generate reactive singlet oxygen that can initiate reaction cascades that result in release of a covalently-linked substrate.[42, 43]

Still, an organic photocage that retains the "plug and play" simplicity that makes *o*-nitrobenzyl photocages so popular but that directly undergoes efficient photorelease using single photons of red/near-IR light rather than UV light would be highly desirable. To that end, a new class of visible light absorbing photocages based on BODIPY dyes were reported by us and Weinstain having strong absorbances >500 nm,

with tunable cellular localization and the ability to manipulate intracellular processes.[44, 45] In collaborative work between our group and the groups of Weinstain and Klan, a structure-reactivity relationship determined that the quantum yields for these green light absorbing BODIPY photocages could be tuned based on substituents, and efficient derivatives were identified.[46] They have since been used in a variety of applications.[47-53] Subsequently, our group showed that increasing the conjugation via appending styryl groups provided BODIPY photocages that absorbed in the far-red/near-IR region of the optical spectrum where mammalian tissues are most transparent (**2-4**).[54] These latter BODIPY photocages are exciting in that they can perform a direct photorelease using single photons of light ~700 nm in this biological window. For example they were recently used by Feringa, Szymanski, and coworkers to control heartbeats using red light.[55] Unfortunately, the low photorelease quantum yields of these structures (Φ_r ~ 0.1%) limits their applicability.

Here, we report new BODIPY photocages having greatly increased photochemical efficiencies over these styryl-substituted derivatives. While the obvious strategy is to develop structures that attempt to improve the efficiency of the desired photorelease reaction, the strategy explored here was to modify the structure to inhibit competitive decay channels by blocking access to unproductive conical intersections (CIs). In the excited state, photochemical partitioning between decay channels is dictated by relative rates. Consequently, the fraction of excited states that channel towards a desired photochemical reaction can be increased simply by inhibiting access to undesired competitive excited state decay channels. New conformationally-restrained BODIPY photocages were synthesized that were hypothesized to block access to these unproductive CIs.

This approach proved to be a highly successful one. In the best case, a 50-fold increase in the quantum efficiencies over the most efficient previously reported structure was achieved, demonstrating that this strategy of inhibiting access to unproductive CIs can be an effective one for improving the efficiency of a desired photoreaction, and providing more efficient photocages that absorb light in the biological window.

Results and Discussion.

Conformational restraint increases quantum yields of photorelease by inhibiting unproductive pathways. Photocages **2**, **3**, and **4**, previously described by our lab[1], have quantum yields of release (Φ_r) of 0.004%, 0.08%, and 0.10%, respectively, with boron-methylation in every case leading to an increase in quantum yield.[4] We hypothesized that the presence of the alkene bonds in structures **2-4** may have resulted in unproductive energy losses due to radiationless decay processes associated with the connecting conformationally free C-C single bonds or *cis-trans* isomerization. Recently, unproductive conical intersections (CIs) for simple BODIPY structures that lead to internal conversion were identified by excited state dynamical simulations and excited state potential energy searches. These include butterflying, charge transfer, B-F scission, and photoisomerization.[56, 57] These pathways are summarized in cartoon form in Figure 2. We anticipated that a conformationally restrained chromophore would make *cis-trans* isomerization impossible, inhibit charge transfer states that prefer twisted geometries,[58] and also help minimize energy losses from the "loose bolt" effect[59] from rotatable C-C single bonds, leading to improved photocages with higher quantum yields of photorelease.

To test the hypothesis, we synthesized ring-fused BODIPY photocages **5-8** and determined their quantum yield of photorelease. These structures take inspiration from the work of Burgess and coworkers[60] on far-red absorbing BODIPY dyes as well as from Schnermann and coworkers on conformational restraint of cyanine dyes.[61, 62] For **5**, the quantum yield is 0.14%, which represents a ~35-fold increase over the comparable boron-fluorinated **2**, and is higher than even than photocage **3** (Φ_r =0.08%) and **4** (Φ_r =0.11%) described in the previous studies that have boron-methylated structures. The boron-methylated derivative **6** has a blue shift in the λ_{max} of 32 nm, but has a substantial ~20-fold increase in quantum yield of the release (Φ_r =2.70%) compared to photocage **5** and a ~30-fold increase compared to structure **3**. The oxidized variant of **6**, photocage **8,** has the highest quantum yield of 3.75%, and a quantum efficiency of 4650 M^{-1} cm^{-1}, which is 50-fold higher than **4**, the best previously-reported[54] photocage absorbing >600 nm. These results suggest conformationally-restrained photocages can inhibit unproductive excited state decay pathways and steer the excited state towards a productive photorelease conical intersection.[63]

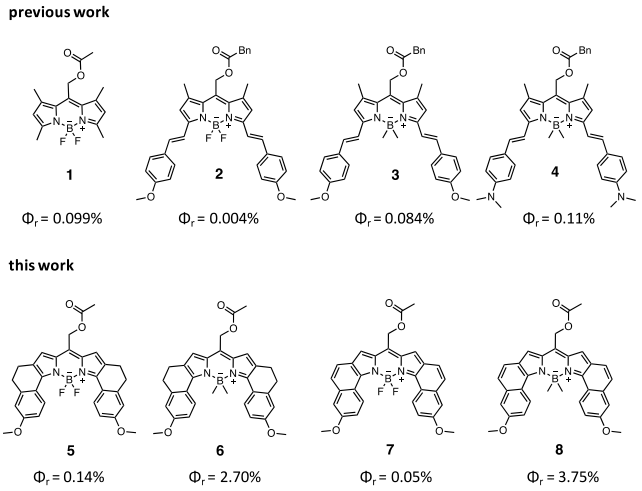

Figure 1. Photocages discussed in the study. Photocages **1-4** are from our previous work while **5-8** are from this work.

Table 1. Photophysical and photochemical properties of **1-15**.

	λ_{abs} (nm)[c]	λ_{em} (nm)[c]	ε (x10^5 $M^{-1}cm^{-1}$)[c]	Φ_r (%)[b]	$\varepsilon\Phi_r$ (M^{-1} cm^{-1})
1[a]	515	526	0.71	0.10	70
2[a]	661	684	0.65	0.004	3
3[a]	647	660	0.49	0.084	41
4[a]	689	728	0.78	0.11	86
5	672	695	1.33	0.14	186

6	641	663	1.39	2.70	3753
7	708	735	1.08	0.05	53
8	681	708	1.24	3.75	4650
9	529	567	0.40	0.18	68
10	673	702	1.46	1.45	2117
11	709	742	0.91	0.22	200
12	642	672	0.90	1.76	1584
13	683	713	1.11	0.22	241
14	672	693	1.21	2.55	3085
15	571	612	0.78	0.08	59

[a] values are from references 44, 46, 54 [b] Quantum yields (Φ_r) determined by quantitative ^{1}H NMR following growth of AcOH using **1** as actinometer (Φ_r=0.099%) in 1:1 $CD_3OD/CDCl_3$ (λ_{ex} = 532 nm, Nd:YAG laser) under air. [c]Absorbance, emission and molar extinction coefficient determined in CH_2Cl_2.

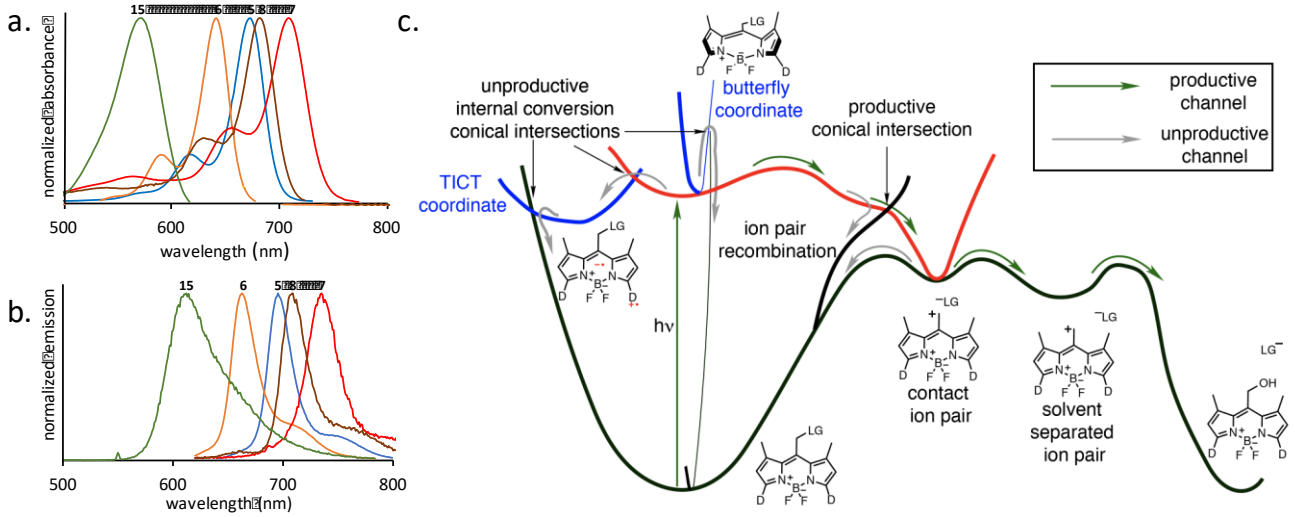

Figure 2. a) Absorption spectra and b) emission spectra of selected photocages in this study (all spectra can be found in the SI). c) A crude pictographic model of the singlet potential energy sufaces showing some possible decay channels.

1,7-Diaryl substitutions improve excited singlet photorelease by excited state participation and blocking ion pair recombination. While conformational restraint is a strategy for blocking unproductive internal conversion intersections, and thereby steering the excited state towards the desired photorelease conical intersection, we also sought to develop ways to prevent energy losses deriving from ground state contact ion pair recombination. To this end, we explored the impact of adding aryl groups in the 1,7-positions adjacent to the BODIPY meso position. We hypothesized that an adjacent nucleophile could trap the nascent carbocation while it was still a contact ion pair, thus preventing ion pair recombination and leading to higher photorelease quantum yields.

Preliminary DFT calculations (B3LYP/6-31G(d), SMD=H_2O) on the singlet carbocation derived from **9** indicate that the free carbocation is not a minimum but undergoes trapping by the adjacent aryl group apparently without a barrier to form the Wheland intermediate. Encouraged by this computational result, we synthesized photocages **9-15**, which have adjacent aryl groups attached to the 1 and 7 positions. In all but one case, these aryl groups lead to an increase in the quantum yield of photorelease compared to the 1,7-dihydro or 1,7-dimethylated derivatives, in some cases significantly. For example, while swapping methyls for phenyls (**1** to **9)** leads to a modest increase in the quantum yield (0.10% to 0.17%, respectively), the increase is larger in the red-light absorbing photocages **5** and **10** (0.14% to 1.45%, respectively).

To evaluate the hypothesis that the increase in quantum yields results from trapping of an intermediate carbocation prior to ion pair cage recombination, analysis of the photolysate of photocage **9**, irradiated in MeOH, was conducted by LC-MS.

These studies revealed the formation of the typical solvent methanol adduct as the major detected product, and the cyclized trapping product as a minor product (Figure 5). Thus, the hypothesized trapping mechanism may explain some of the increase in quantum yield for these derivatives, but seems unlikely to fully explain the sometimes dramatic increase in the quantum yield, such as the 10-fold increase in quantum yield for **10** relative to **5.** Either the computations suggesting a barrierless trapping by the adjacent aryl groups are wrong (that is, there is in reality some barrier for the adjacent aryl ring to attack the carbocation, leading to competitive trapping between the solvent and the aryl ring), or the photoreaction never generates a fully free carbocation (i.e., solvent trapping is nearly concerted with leaving group release).

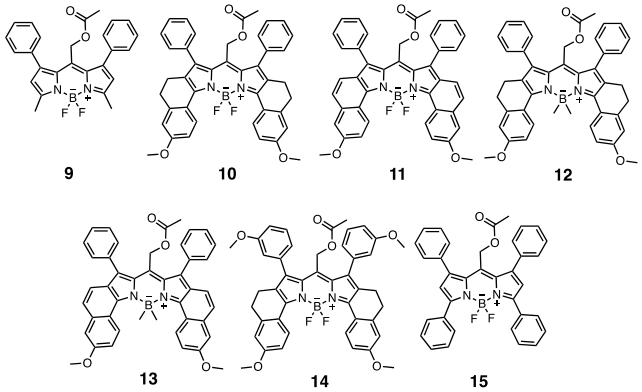

Figure 3. New 1,7 diaryl derivatives synthesized for this study designed to inhibit ion pair recombination by internal trapping.

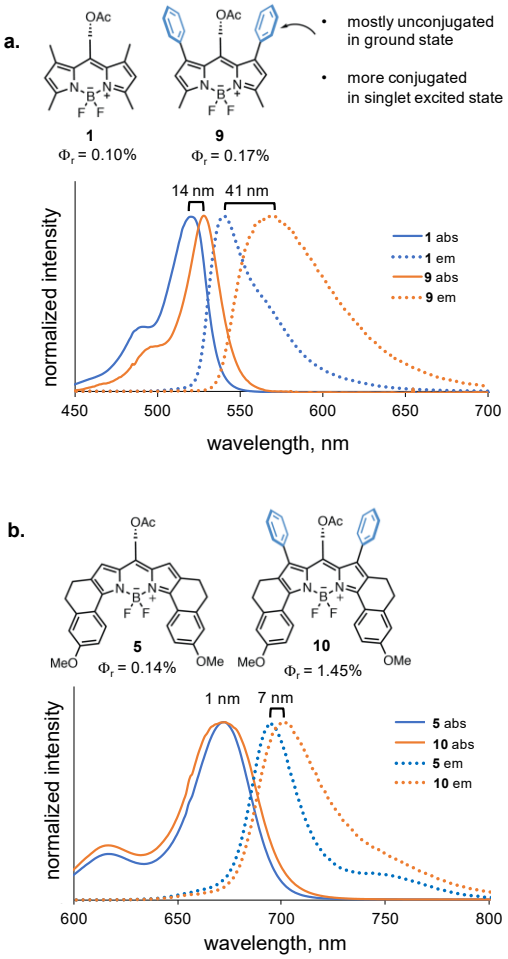

Figure 4. Absorption and emission spectra of **1**,**9** and **5**,**10** demonstrating greater participation of 1,7-diaryl groups in the excited state than the ground state.

Several pieces of evidence suggest that the adjacent aryl groups also impact the singlet excited state photochemistry, and are not entirely just involved following the formation of the solvent-caged ion pair and return to the ground state. Inspection of the absorption and emission profiles of these photocages shows that the adjacent aryl rings are mostly unconjugated in the ground state, as the derivatives with 1,7-dimethyl or 1,7-dihydro groups has nearly the same λ_{max} as the 1,7-diaryl derivatives. This observation is also supported by DFT computations of the optimized geometries of these photocages in the ground state, with the aryl rings adopting a nearly perpendicular conformation relative to the BODIPY chromophore (see SI S55-S60). While the ground state absorption is largely unaffected by the adjacent aryl rings, the fluorescence emission is red-shifted in the 1,7-diaryl derivatives. For example, **9** has a red-shifted emission by 41 nm compared to **1**, while **10** has a red-shifted emission of 9 nm relative to **5** (See Figure 4). This result suggests increased participation of the aryl rings in the singlet excited state, and a shift of one or both of the aryl rings to a more conjugated conformation. This finding is not so unusual, as biaryls like biphenyl are often twisted in the ground state and planar in the excited state.

Further evidence that there is an electronic component to the increase in quantum yields and not solely a steric effect comes from a comparison of photocages **10** and **14 (Figure 5)**. Photocage **14** has a more electron rich anisyl ring, making it a better nucleophile, and this derivative has a higher quantum yield of photorelease than the phenyl derivative. The methoxy group in the meta position is not expected to have a large steric impact on ion pair recombination. Because the fluorescence data indicate that the 1,7-diaryl substituents participate in the excited state, but not the ground state, the adjacent aryl groups may act to lower the barrier for photorelease by mixing into the excited state wavefunction at the bond-breaking transition state. It is also possible that they provide a steric barrier for ion pair recombination. Bond cleavage on the triplet excited state suggests a concerted slide of the phenyl groups into a wing-like conformation that may block anion return.

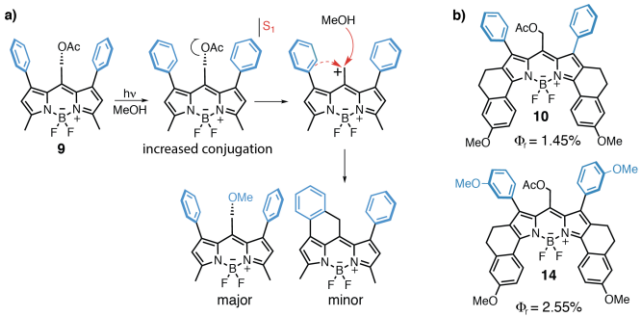

Figure 5. a) Photoproducts of **9** detected using LC-MS b) Increase in quantum yield upon introducing electron-donating group to **1**,**7**-diaryl groups.

In contrast, 1,7-diarylation seems to have little effect on photorelease from the triplet excited state. In the triplet excited state, a simple photo-S_N1 reaction would lead to a triplet carbocation. Unlike on the singlet surface, ion pair recombination is then spin forbidden.[63,64] While trapping of the carbocation by the adjacent aryl group is computed to be barrierless on the singlet surface, a substantial barrier for trapping is computed on the triplet surface. A potential energy scan of the C-O bond stretch for **5**, **7**, **10**, **11** on the triplet surface (B3LYP/6-31G(d), SMD=H_2O), leads to identical barriers for the 1,7-dihydro derivative vs. the 1,7-diaryl derivative. Overall, these results suggest that 1,7-diaryl substitutions benefit photorelease on the singlet excited state, but have little effect on photorelease occurring on the triplet excited state.

Benefit of boron-methylation decreases as excited singlet photorelease is improved. Adjacent 1,7-diaryl substitutions lead to large improvements in the quantum yields for photocages featuring boron-fluorination, while with the B-methylated photocages the improvements are smaller and, in one case, deleterious (**13** vs **8**). Alkylation of BODIPY photocages has recently been shown to dramatically improve photorelease quantum yields.[46, 50] Part of the increase can be assigned to B-methylation promoting intersystem crossing to a longer-lived triplet state. This was recently observed by the B-alkylated photocage byproduct acting as a better singlet oxygen photosensitizer than methylene blue.[51] Alkylated BODIPY photocages also have lower computed electronic barriers for heterolysis.[46] With good leaving groups like chloride, photorelease on the triplet excited state is energetically favored and nearly barrierless.[46]

Often, an increase in intersystem crossing quantum yield to the triplet state is marked by a decrease in the fluorescence quantum yield. Indeed, we observed that boron-methylated photocage **12** has a quantum yield of fluorescence of 0.17 compared to 0.39 for B-fluorinated photocage **10**, which supports the idea that boron alkylation promotes intersystem crossing.

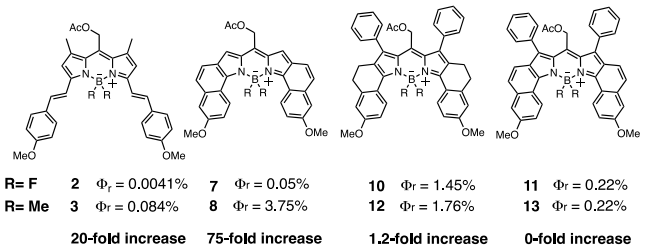

Figure 6. Effect of alkylation in 1,7-diarylated and non-arylated structures.

However, as can be seen in Figure 6, the impact of boron-methylation is large in some cases, but minimal in others. We found that there is no change in the computed energy barrier for C-O bond cleavage in the triplet excited state when adding phenyl groups at the 1,7-positions. This computational result further supports the idea that alkylation promotes intersystem crossing. Likely, the benefits for the 1,7-diaryl derivatives derives mostly from improving productive photorelease on the excited singlet surface rather than the excited triplet surface. Importantly, there is a notable drop in the effect of boron-alkylation on quantum yield when the adjacent phenyl group is present. This suggests that as the singlet photochemistry is improved, the beneficial effect of boron methylation becomes less pronounced, likely as a consequence of diminished benefit of triplet photorelease relative to singlet excited state photorelease.

Photoactivation in cells and toxicity evaluation. To evaluate whether these new derivatives can cross cell membranes, are non-toxic, and undergo photorelease in living cells, we synthesized **16** with a 4-nitrobenzoic acid leaving group. 4-Nitrobenzoic acid is a known quencher of BODIPY dyes. We anticipated that, upon irradiation, photorelease of the quencher should lead to a solvent adduct of the BODIPY photocage with a higher fluorescence that could be monitored by fluorescence microscopy, allowing us to visualize photorelease in cells. Indeed, a slow increase in fluorescence occurs (Figure S5) when the solution of **16** is irradiated.

Further studies were performed (Figure 7) in HeLa cells incubated with compound **16** at 37 °C for 30 minutes. After incubation, the cells were irradiated with 635 ± 20 nm light, and the fluorescence emission was measured at 690 ± 30 nm. Prior to irradiation, we observed a low background fluorescence after incubation. An increase in fluorescence was observed at 690 nm when the cells were irradiated. In control studies, there was no such increase in the fluorescence intensity in the absence of irradiation. Cytotoxicity studies using the Trypan blue exclusion assay show no decrease in viability of cells with the treatment of compound **16** (93±4%) compared to the non-treated cells (94±5%) at 20 μM.

EXPERIMENTAL

Determination of quantum yield of photorelease. The quantum yield of release was determined by using BODIPY **1** as the actinometer in deuterated methanol solvent. The release of acetic acid was followed using quantitative ^{1}H NMR. For quantitative accuracy, a 90° pulse angle was used along with 20 seconds of recycling delay cycle. The sample was irradiated in 3 mL cuvette using a 532 nm Nd: YAG laser. Dimethyl sulfone was used as the internal standard, and quantifying the release of acetic acid was determined relative to this internal standard. (A full procedure is found in the supporting information).

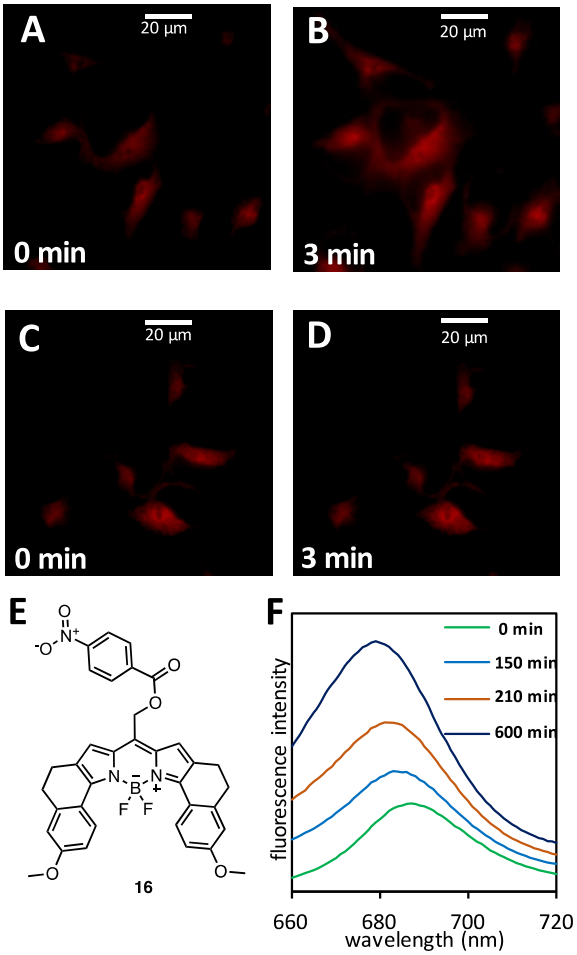

Figure 7. Fluorescence images of (A and B) HeLa cells incubated with 20 μM **16** irradiated with 635 nm light and (C and D) cell incubated with **16** without irradiation (Control). F is the change in fluorescence intensity of compound **16** in solution of 1:1 CH_2Cl_2/ Methanol on irradiation with halogen lamp.

Cell studies. The human cervical carcinoma (HeLa) cell line was used to study the photoactivation of compound **16**. Dulbecco's Modified Eagle Medium (DMEM) supplemented with 10% fetal bovine serum, 12.5 mM streptomycin, and 36.5 mM penicillin was used as the culture medium. Cells were maintained at 37 ^{o}C in a water jacketed incubator with 5% CO_2 supply. Cells grown on custom-made glass-bottom dishes were used for the microscopy experiments. On the day of the microscopy studies, the culture medium was replaced with 20 μM **16** in the serum-free DMEM medium. Cells were then incubated at 37 ^{o}C for 30 minutes, rinsed three times with HEPES imaging buffer (pH=7.2, 155 mM NaCl, 5 mM KCl, 2 mM $CaCl_2$, 1 mM $MgCl_2$, 2 mM NaH_2PO_4, 10 mM HEPES and 10 mM Glucose) and used for imaging.

Microscopy studies. Fluorescence imaging experiments were performed on a Nikon Eclipse TE2000U microscope (Melville, NY) operating in wide-field, epi-fluorescence mode. The irradiation light from a mercury lamp (X-cite 120 PC, EXFO Photonic Solutions Inc, Canada) was filtered using a 635 ±20 nm filter, and projected to the cell samples through a 100×Apo, 1.49-numerical aperture oil-immersion objective. Fluorescence emission was filtered through a 690 ± 30 nm filter and images were collected using a PhotonMAX 512 EMCCD camera (Princeton Instruments, NJ). To demonstrate the photoactivation of compound **16** in cells, the sample was irradiated continuously, and images were collected every 30 seconds with 100 ms acquisition time per image. For the control experiment, a cell sample treated with compound **16** was maintained in dark and irradiated with 635 ±20 nm light only for a short period (100ms) to collect the images in 30 second intervals. Images were further analyzed with the ImageJ program (National Institute of Health).

Cytotoxicity studies. Trypan blue exclusion assay was used to determine the cytotoxicity of **16** in Hela cells. Cells were treated with 20 μM **16** in the DMEM medium. After a 30 minute incubation period, equal volumes of trypsinized cell suspension and 0.4 % Trypan blue dye were mixed in a vial and incubated at room temperature for 2 minutes. The viable cell count (cells that excluded the dye) was determined using a hemacytometer and an optical microscope. There was no significant difference in cell viability observed for the **16** treated cells (93 ± 4 %) compared to the non-treated cells (94 ± 5 %).

CONCLUSION

We have identified new far-red/near-IR absorbing BODIPY-based photocages that have superior quantum efficiencies to the "first-generation" BODIPY photocages absorbing >600 nm. In the best case, the quantum efficiencies are >50 times larger than the best previously identified one. On a practical note, while photocage **8** has the highest quantum yield of the derivatives studied, we noticed that this chromophore was challenging to manipulate synthetically. Photocage **6** is more robust, easier to make, can be easily hydrolyzed to the alcohol to allow functionalization with a desired biological leaving group, and has nearly the same quantum yield (2.7% for **6** vs. 3.8% for **8**). It also absorbs maximally at ~640 nm, close to a common current photodynamic therapy excitation source of 630 nm. This derivative may prove to an attractive alternative.

The low single-digit quantum yields of the best of these derivatives are slightly lower than the parent nitrobenzyl photocage, but about the same as the popular dimethoxynitrobenzyl derivatives. On the other hand, these BODIPY photocages absorb strongly in the biological window ($\varepsilon >$ 100,000 $M^{-1}cm^{-1}$), so the resulting quantum efficiencies are about an order of magnitude higher than the nitrobenzyl photocages. These new BODIPY photocages hold the promise of allowing the same kind of "plug and play" simplicity that makes the nitrobenzyl photocages so popular—just tack on your biological leaving group and irradiate with red light to pop it off. This can be achieved with a laser, with widely available red LEDs, or practically any visible light source (for crude studies, we use a 500W halogen lamp, purchased cheaply from a home-supply store, with a beaker of water as an IR cutoff filter to prevent heating the sample). Consequently, for studies requiring deep-tissue penetration or phototherapeutics, these new photocages are an attractive addition to the photocage arsenal.

ASSOCIATED CONTENT

Supporting Information

Synthetic procedures, compound characterization data, all UV-Vis and emission spectra, full procedures for determining quantum yields of fluorescence and photorelease, computational coordinates and absolute energies.

The Supporting Information is available free of charge on the ACS Publications website.

AUTHOR INFORMATION

Corresponding Author

* winter@iastate.edu, esmith1@iastate.edu

ACKNOWLEDGMENT

A.H.W. thanks the National Science Foundation (CHE-1464956) and Bailey Award for support. E.A.S. thanks the National Science Foundation (CHE-1709099).

REFERENCES

1. Klan, P.; Solomek, T.; Bochet, C. G.; Blanc, A.; Givens, R.; Rubina, M.; Popik, V.; Kostikov, A.; Wirz, J., Photoremovable Protecting Groups in Chemistry and Biology: Reaction Mechanisms and Efficacy. *Chem. Rev.* **2013,** *113*, 119.
2. Pirrung, M. C., Spatially Addressable Combinatorial Libraries. *Chem. Rev.* **1997,** *97*, 473.
3. Kretschy, N.; Holik, A. K.; Somoza, V.; Stengele, G. P.; Somoza, M. M., Next-Generation o-Nitrobenzyl Photolabile Groups for Light-Directed Chemistry and Microarray Synthesis. *Angew. Chem., Int. Ed.* **2015,** *54*, 8555.
4. Katz, J. S.; Burdick, J. A., Light-Responsive Biomaterials: Development and Applications. *Macromol. Biosci.* **2010,** *10*, 339.
5. Wuts, P. G. M.; Greene, T. W., *Greene's Protective Groups in Organic Synthesis*. Wiley: 2012.
6. Lawrence, D. S., The preparation and in vivo applications of caged peptides and proteins. *Curr. Opin. Chem. Biol.* **2005,** *9*, 570.

7. Zhao, J.; Lin, S.; Huang, Y.; Chen, P. R., Mechanism-Based Design of a Photoactivatable Firefly Luciferase. *J. Am. Chem. Soc.* **2013,** *135* (20), 7410.
8. Kaplan, J. H.; Forbush, B.; Hoffman, J. F., Rapid photolytic release of adenosine 5'-triphosphate from a protected analog: utilization by the sodium:potassium pump of human red blood cell ghosts. *Biochemistry* **1978,** *17* (10), 1929-1935.
9. Walbert, S.; Pfleiderer, W.; Steiner, U. E., Photolabile Protecting Groups for Nucleosides: Mechanistic Studies of the 2-(2-Nitrophenyl)ethyl Group. *Helvetica Chimica Acta* **2001,** *84* (6), 1601-1611.
10. Walker, J. W.; Reid, G. P.; McCray, J. A.; Trentham, D. R., Photolabile 1-(2-nitrophenyl)ethyl phosphate esters of adenine nucleotide analogs. Synthesis and mechanism of photolysis. *J. Am. Chem. Soc.* **1988,** *110* (21), 7170-7177.
11. Mbatia, H. W.; Bandara, H. M. D.; Burdette, S. C., CuproCeav-1, a first generation photocage for Cu+. *Chem. Commun.* **2012,** *48*, 5331.
12. Atilgan, A.; Eaik, E. T.; Guliyev, R.; Uyar, T. B.; Erbas-Cakmak, S.; Akkaya, E. U., Near-IR-Triggered, Remote-Controlled Release of Metal Ions: A Novel Strategy for Caged Ions. *Angew. Chem., Int. Ed.* **2014,** *53* (40), 10678.
13. Kaplan, J. H.; Ellis-Davies, G. C. R., Photolabile chelators for the rapid photorelease of divalent cations. *Proc. Natl. Acad. Sci. U. S. A.* **1988,** *85*, 6571.
14. Gomez, T. M.; Spitzer, N. C., In vivo regulation of axon extension and pathfinding by growth-cone calcium transients. *Nature* **1999,** *397* (28), 350.
15. Brown, E. B.; Shear, J. B.; Adams, S. R.; Tsien, R. Y.; Webb, W. W., Photolysis of caged calcium in femtoliter volumes using two-photon excitation. *Biophys. J.* **1999,** *76*, 489.
16. Kramer, R. H.; Chambers, J. J.; Trauner, D., Photochemical tools for remote control of ion channels in excitable cells. *Nat. Chem. Biol.* **2005,** *1* (7), 360.
17. Ellis-Davies, G. C. R., Caged compounds: photorelease technology for control of cellular chemistry and physiology. *Nat. Methods* **2007,** *4* (8), 619.
18. Adams, S. R.; Tsien, R. Y., Controlling cell chemistry with caged compounds. *Annu. Rev. Physiol.* **1993,** *55*, 755.
19. Lin, Q.; Huang, Q.; Li, C.; Bao, C.; Liu, Z.; Li, F.; Zhu, L., Anticancer Drug Release from a Mesoporous Silica Based Nanophotocage Regulated by either a one- or two-photon process. *J. Am. Chem. Soc.* **2010,** *132* (31), 10645.
20. Liu, M.; Meng, J.; Bao, W.; Liu, S.; Wei, W.; Ma, G.; Tian, Z., Single-Chromophore-Based Therapeutic Agent Enables Green-Light-Triggered Chemotherapy and Simultaneous Photodynamic Therapy to Cancer Cells. *ACS Applied Bio Materials* **2019,** *2* (7), 3068-3076.
21. Li, W. h.; Zheng, G., Photoactivatable fluorophores and techniques for biological imaging applications. *Photochem. Photobiol. Sci.* **2012,** *11*, 460.
22. Puliti, D.; Warther, D.; Orange, C.; Specht, A.; Goeldner, M., Small photoactivatable molecules for controlled fluorescence activation in living cells. *Bioorg. Med. Chem.* **2011,** *19* (3), 1023.
23. Mayer, G.; Heckel, A., Biologically Active Molecules with a "Light Switch". *Angew. Chem., Int. Ed.* **2006,** *45* (30), 4900-4921.
24. Goeldner, M.; Givens, R., *Dynamic Studies in Biology: Phototriggers, Photoswitches and Caged Biomolecules*. Wiley: 2006.
25. Park, C. H.; Givens, R. S., New Photoactivated Protecting Groups. 6. p-Hydroxyphenacyl: A Phototrigger for Chemical and Biochemical Probes. *J. Am. Chem. Soc.* **1997,** *119* (10), 2453.
26. Ackmann, A. J.; Frechet, M. J., The generation of hydroxide and methoxide ions by photo-irradiation: use of aromatization to stabilize ionic photo-products from acridine derivatives. *Chem. Commun.* **1996,** *5*, 605.
27. Givens, R. S.; Matuszewski, B., *J. Am. Chem. Soc.* **1984,** *106*, 6860.
28. Olson, J. P.; Banghart, M. R.; Sabatini, B. L.; Ellis-Davies, G. C. R., Spectral Evolution of a Photochemical Protecting Group for Orthogonal Two-Color Uncaging with Visible Light. *J. Am. Chem. Soc* **2013,** *135* (42), 15948-15954.
29. Antony, L. A. P.; Slanina, T.; Sebej, P.; Solomek, T.; Klan, P., Fluorescein Analogue Xanthene-9-Carboxylic Acid: A Transition-Metal-Free CO Releasing Molecule Activated by Green Light. *Org. Lett.* **2013,** *15* (17), 4552.
30. Sharma, R.; Knoll, J. D.; Martin, P. D.; Podgorski, I.; Turro, C.; Kodanko, J. J., Ruthenium Tris(2-pyridylmethyl)amine as an Effective Photocaging Group for Nitriles. *Inorg. Chem.* **2014,** *53* (7), 3272-3274.
31. Arumugam, S.; Popik, V. V., Photochemical generation and the reactivity of o-naphthoquinone methides in aqueous solutions. *J. Am. Chem. Soc.* **2009,** *131* (33), 11892.
32. Aujard, I.; Benbrahim, C.; Gouget, M.; Ruel, O.; Baudin, J.-B.; Neveu, P.; Jullien, L., o-Nitrobenzyl Photolabile Protecting Groups with Red-Shifted Absorption: Syntheses and Uncaging Cross-Sections for One- and Two-Photon Excitation. *Chem. Eur. J.* **2006,** *12* (26), 6865-6879.
33. Jakkampudi, S.; Abe, M., Caged Compounds for Two-Photon Uncaging. In *Reference Module in Chemistry, Molecular Sciences and Chemical Engineering*, Elsevier: 2018.
34. Tran, C.; Gallavardin, T.; Petit, M.; Slimi, R.; Dhimane, H.; Blanchard-Desce, M.; Acher, F. C.; Ogden, D.; Dalko, P. I., Two-photon caging groups: effect of position isomery on the photorelease properties of aminoquinoline-derived photolabile protecting groups. *Org. Lett.* **2015,** *17* (3), 402.
35. Denning, D. M.; Pedowitz, N. J.; Thum, M. D.; Falvey, D. E., Uncaging alcohols using uv or visible light photoinduced electron transfer to 9-phenyl-9-tritylone ethers. *Org. Lett.* **2015,** *17* (24), 5986.
36. Falvey, D. E.; Sundararajan, C., Photoremovable protecting groups based on electron transfer chemistry. *Photochem. Photobiol. Sci.* **2004,** *3*, 831.
37. Sundararajan, C.; Falvey, D. E., Alkylpicolinium Esters using photosensitization by high wavelength laser dyes. *J. Am. Chem. Soc.* **2005,** *127* (22), 8000.
38. Priestman, M. A.; Lawrence, D. S., Light-Mediated Remote Control of Signaling Pathways. *Biochim. Biophys. Acta, Proteins Proteomics* **2010,** *1804* (3), 547.
39. Shell, T. A.; Shell, J. R.; Rodgers, Z. L.; Lawrence, D. S., Tunable visible and near-ir photoactivation of light-responsive compounds by using fluorophores as light-capturing antennas. *Angew. Chem., Int. Ed.* **2014,** *53* (3), 875.
40. Wang, X.; Kalow, J. A., Rapid Aqueous Photouncaging by Red Light. *Org. Lett.* **2018,** *20* (7), 1716.
41. Walton, D. P.; Dougherty, D. A., A General Strategy for Visible-Light Decaging Based on the Quinone Trimethyl Lock. *J. Am. Chem. Soc.* **2017,** *139* (13), 4655-4658.
42. Nani, R. R.; Gorka, A. P.; Nagaya, T.; Kobayashi, H.; Schnermann, M. J., Near-IR Light-Mediated Cleavage of Antibody-Drug Conjugates Using Cyanine Photocages. *Angew. Chem.* **2015,** *127* (46), 13839.
43. Gorka, A. P.; Nani, R. R.; Schnermann, M. J., Harnessing Cyanine Reactivity for Optical Imaging and Drug Delivery. *Acc. Chem. Res.* **2018,** *51* (12), 3226-3235.

44. Goswami, P.; Syed, A.; Beck, C. L.; Albright, T. R.; Mahoney, K. M.; Unash, R.; Smith, E. A.; Winter, A. H., BODIPY-Derived Photoremovable Protecting Groups Unmasked with Green Light. *J. Am. Chem. Soc.* **2015,** *137*, 3783.
45. Rubinstein, N.; Liu, P.; Miller, E. W.; Weinstain, R., meso-Methylhydroxy BODIPY: a scaffold for photo-labile protecting groups. *Chem. Commun.* **2015,** *51*, 6369.
46. Slanina, T.; Shrestha, P.; Palao, E.; Kand, D.; Peterson, J. A.; Dutton, A. S.; Rubinstein, N.; Weinstain, R.; Winter, A. H.; Klan, P., In Search of the Perfect Photocage: Structure Reactivity Relationships in meso-Methyl BODIPY Photoremovable Protecting Groups. *J. Am. Chem. Soc.* **2017,** *139* (42), 15168-15175.
47. Lv, W.; Wang, W., One-Photon Upconversion-Like Photolysis: A New Strategy to Achieve Long-Wavelength Light-Excitable Photolysis. *Synlett* (EFirst).
48. Li, M.; Dove, A. P.; Truong, V. X., Additive-Free Green Light-Induced Ligation Using BODIPY Triggers. *Angew. Chem., Int. Ed.* **2020,** *59* (6), 2284-2288.
49. Sitkowska, K.; Feringa, B. L.; Szymański, W., Green-Light-Sensitive BODIPY Photoprotecting Groups for Amines. *J. Org. Chem.* **2018,** *83* (4), 1819.
50. Peterson, J. A.; Fischer, L. J.; Gehrmann, E. J.; Shrestha, P.; Yuan, D.; Wijesooriya, C. S.; Smith, E. A.; Winter, A. H., Direct Photorelease of Alcohols from Boron-Alkylated BODIPY Photocages. *J. Org. Chem.* **2020,** *85* (8), 5712-5717.
51. Toupin, N. P.; Arora, K.; Shrestha, P.; Peterson, J. A.; Fischer, L. J.; Rajagurubandara, E.; Podgorski, I.; Winter, A. H.; Kodanko, J. J., BODIPY-Caged Photoactivated Inhibitors of Cathepsin B Flip the Light Switch on Cancer Cell Apoptosis. *ACS chemical biology* **2019,** *14* (12), 2833-2840.
52. Kand, D.; Liu, P.; Navarro, M. X.; Fischer, L. J.; Rousso-Noori, L.; Friedmann-Morvinski, D.; Winter, A. H.; Miller, E. W.; Weinstain, R., Water-Soluble BODIPY Photocages with Tunable Cellular Localization. *J. Am. Chem. Soc* . **2020,** *142* (11), 4970-4974.
53. Kand, D.; Pizarro, L.; Angel, I.; Avni, A.; Friedmann-Morvinski, D.; Weinstain, R., Organelle-Targeted BODIPY Photocages: Visible-Light-Mediated Subcellular Photorelease. *Angew. Chem., Int. Ed.* **2019,** *58* (14), 4659-4663.
54. Peterson, J. A.; Wijesooriya, C.; Gehrmann, E. J.; Mahoney, K. M.; Goswami, P. P.; Albright, T. R.; Syed, A.; Dutton, A. S.; Smith, E. A.; Winter, A. H., Family of BODIPY Photocages Cleaved by Single Photons of Visible/Near-Infrared Light. *J. Am. Chem. Soc.* **2018,** *140* (23), 7343-7346.
55. Sitkowska, K.; Hoes, M. F.; Lerch, M. M.; Lameijer, L. N.; van der Meer, P.; Szymański, W.; Feringa, B. L., Red-light-sensitive BODIPY photoprotecting groups for amines and their biological application in controlling heart rhythm. *Chem. Commun.* **2020,** *56* (41), 5480-5483.
56. Lin, Z.; Kohn, A. W.; Van Voorhis, T., Toward Prediction of Nonradiative Decay Pathways in Organic Compounds II: Two Internal Conversion Channels in BODIPYs. *J. Phys. Chem.C* **2020,** *124* (7), 3925-3938.
57. Briggs, E. A.; Besley, N. A.; Robinson, D., QM/MM Excited State Molecular Dynamics and Fluorescence Spectroscopy of BODIPY. *J. Phys. Chem. A* **2013,** *117* (12), 2644-2650.
58. Hoelzel, C. A.; Hu, H.; Wolstenholme, C. H.; Karim, B. A.; Munson, K. T.; Jung, K. H.; Zhang, H.; Liu, Y.; Yennawar, H. P.; Asbury, J. B.; Li, X.; Zhang, X., A General Strategy to Enhance Donor-Acceptor Molecules Using Solvent-Excluding Substituents. *Angew. Chem., Int. Ed.* **2020,** *59* (12), 4785-4792.
59. Turro, N. J., *Modern Molecular Photochemistry*. University Science Books: 1991.
60. Chen, J.; Burghart, A.; Derecskei-Kovacs, A.; Burgess, K., 4,4-Difluoro-4-bora-3a,4a-diaza-s-indacene (BODIPY) Dyes Modified for Extended Conjugation and Restricted Bond Rotations. *J. Org. Chem. y* **2000,** *65* (10), 2900-2906.
61. Michie, M. S.; Götz, R.; Franke, C.; Bowler, M.; Kumari, N.; Magidson, V.; Levitus, M.; Loncarek, J.; Sauer, M.; Schnermann, M. J., Cyanine Conformational Restraint in the Far-Red Range. *J. Am. Chem. Soc.* **2017,** *139* (36), 12406-12409.
62. Matikonda, S. S.; Hammersley, G.; Kumari, N.; Grabenhorst, L.; Glembockyte, V.; Tinnefeld, P.; Ivanic, J.; Levitus, M.; Schnermann, M. J., Impact of Cyanine Conformational Restraint in the Near-Infrared Range. *J. Org. Chem.* **2020,** *85* (9), 5907-5915.
63. Buck, A.; Beck, C.; Winter, A., Inverted Substrate Preferences for Photochemical Heterolysis Arise from Conical Intersection Control. *J. Am. Chem. Soc.* **2014,** *136* (25), 8933-8940.
64. Albright, T.; Winter, A., A Fine Line Separates Carbocations from Diradical Ions in Donor-Unconjugated Cations. *J. Am. Chem. Soc.* **2015,** *137* (9), 3402-3410.

TOC GRAPHIC: